4ICEGE Thessaloniki-GREECE 2007

4th International Conference on
Earthquake Geotechnical Engineering
June 25-28, 2007
Paper No. 1550

PSEUDOSTATIC AND DYNAMIC ANALYSES OF TUNNELS IN TRANSVERSAL AND LONGITUDINAL DIRECTIONS

Emilio BILOTTA[1], Giovanni LANZANO[2], Gianpiero RUSSO[3], Filippo SANTUCCI de MAGISTRIS[4], Vincenzo AIELLO[5], Enrico CONTE[6], Francesco SILVESTRI[7], Michele VALENTINO[8]

ABSTRACT

Effects induced by earthquakes in a tunnel lining can be assessed with several methods at increasing levels of complexity, by evaluating the load increments from a free-field seismic response analysis, or after the solution of a dynamic soil-structure interaction problem. In this paper, different procedures are shown and their results are compared. The sample problem was a circular tunnel of 6 m in diameter and 1000 m long, with the axis at a depth of 15 m in a 30 m thick layer of medium dense gravel, sand or soft clay, overlying relatively stiff bedrock. Pseudo-static and simplified dynamic analyses have been performed and compared with a full dynamic soil-structure interaction analysis, carried out by the finite element method. Results show that as far as the structure is relatively flexible, simplified methods can be used to reliably assess the seismic forces induced on the tunnel. Nevertheless, the straightforward pseudo-static analyses need a careful evaluation of the surface acceleration. Along the longitudinal axis two procedures have been compared, which can take into account, in a simplified way, both the obliquity of seismic waves and the non-synchronism of the motion.

Keywords: underground structures, tunnels, seismic loads, pseudo-static analysis, dynamic analysis

INTRODUCTION

It was common opinion that earthquake effects on underground structures are not very important. This is because these structures have generally experienced a low level of damage in comparison to constructions above ground. Nevertheless, some underground facilities were significantly damaged during recent strong earthquakes (Hashash et al., 2001). As a consequence of this, and owing to the increasing protection level needed in constructing large-diameter tunnels especially in urban areas, the seismic response of these structures have been addressed by many authors in the last years (St.John & Zahrah, 1987; Wang 1993; Kawashima, 2000; Vanzi, 2000; Hashash, 2005; Pakbaz & Yareevand, 2005).

[1] Research Assistant, DIG, University of Napoli Federico II, Italy, Email: bilotta@unina.it
[2] PhD Student, DIG, University of Napoli Federico II, Italy, Email g.lanzano@unina.it
[3] Associate Professor, DIG, University of Napoli Federico II, Italy, Email: gianpiero.russo@unina.it
[4] Research Associate, SAVA, University of Molise, Italy, Email: filippo.santucci@unimol.it
[5] Research Assistant, DDS, University of Calabria, Italy Email: v.aiello@dds.unical.it
[6] Associate Professor, DDS, University of Calabria, Italy Email: conte@dds.unical.it
[7] Professor, DDS, University of Calabria, Italy Email: f.silvestri@unical.it
[8] Research Student, DDS, University of Calabria, Italy: omegamiky@yahoo.it

Earthquake damages of underground structures are due to ground shaking and soil failures such as liquefaction or slope instabilities. In particular, the response of tunnels to earthquake motion, which is the topic of the present work, appears in three forms of deformation: axial compression and extension, longitudinal bending and ovaling/racking (Owen & Scholl, 1981). Axial and bending deformations are generated by the components of seismic waves producing particle motion parallel or perpendicular to the longitudinal axis of the tunnel, respectively. Ovaling or racking deformations are mostly due to shear waves propagating perpendicularly to the tunnel axis, resulting in a distortion of the cross-section of the structure. Generally, these different forms of deformation are analysed separately. Specifically, design considerations are in the direction along the tunnel axis for axial and bending deformations, and in transverse direction for ovaling deformation.

In this paper, forces induced by ground shaking in the tunnel lining are evaluated using several calculation procedures at different levels of complexity, which fall into the class of the pseudo-static and simplified dynamic methods (Rampello, 2005). Results obtained modelling complete dynamic soil-structure interaction are also shown. The case of a circular tunnel embedded in soil deposit overlying relatively stiff bedrock is analysed. Three different subsoil models are considered: a layer of soft clay, medium dense sand or gravel. In addition, many acceleration time histories registered in Italy during seismic events are employed as input motion. The free-field soil deformations caused by wave propagation are calculated under the assumption that the soil behaviour is described by a linear or nonlinear visco-elastic model. The interaction of the underground structure with the surrounding soil is analysed both in transversal and longitudinal directions.

REFERENCE SUBSOIL MODELS

The analytical simulations have been performed on three idealized ground conditions (Fig. 1): a 30 m thick layer of soft clay, medium dense sand or gravel, overlying a soft rock half-space as a bedrock (V_r= 800 m/s, γ=22 kN/m^3, D_o=0.5%). The tunnel has the following characteristics:

- circular shape with reinforced concrete lining (thickness t=0.3 m, diameter D=6 m);
- axis depth z_o=15 m, length 1000 m.

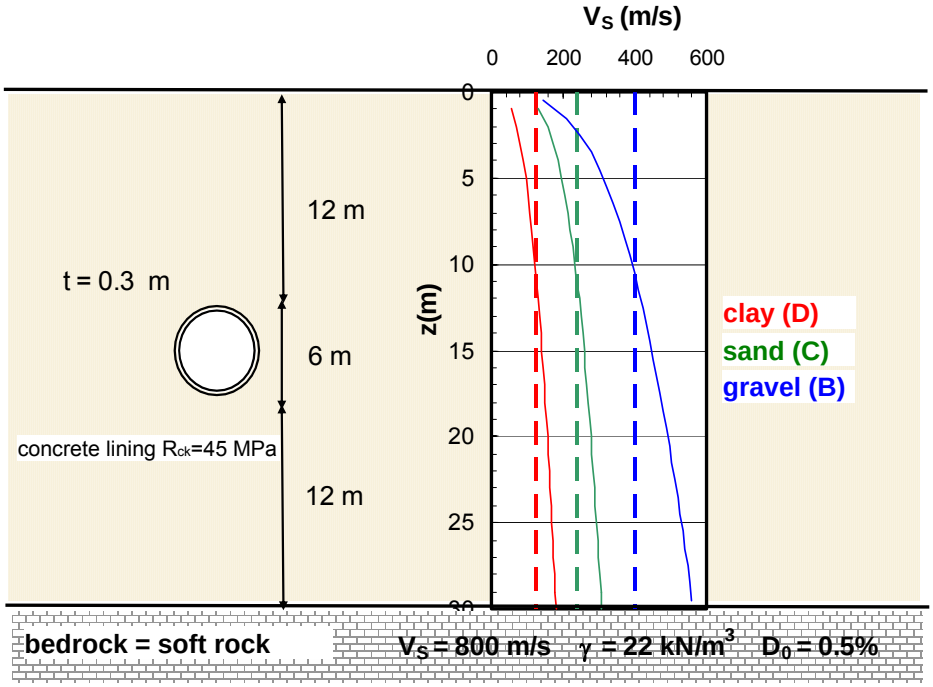

Figure 1. Subsoil models

The values of small strain soil parameters have been chosen by means of literature empirical relationships, linking the shear modulus (G_o) and the damping ratio (D_0) to the lithostatic stress, the void ratio and intrinsic soil properties, such as particle size and plasticity index I_P (Santucci de Magistris, 2005; d'Onofrio & Silvestri, 2001). Starting from $G_o(z)$, it is possible to obtain the shear wave velocity profile $V_s(z)$ as:

$$V_s(z) = \sqrt{\frac{G_0(z)}{\rho}} \tag{1}$$

where ρ is the soil density. The variations of V_s with depth for each soil model are shown in Fig. 1, where the dashed lines represent the value of the so called 'equivalent velocity' (EN 1998-1, 2003):

$$V_{s,30} = \frac{30}{\sum_{i=1,n} h_i / V_{s,i}} \tag{2}$$

Table 1 summarizes the geotechnical parameters, the ground type according to the Italian code (OPCM 3274, 2003), and the corresponding values for the site amplification factor, S.

Table 1: Ground parameters and classification according to OPCM 3274

Ground	φ'(°)	I_P(%)	γ(kN/m^3)	D_0(%)	$V_{S,30}$(m/s)	Type	S
Clay	25	30	18	2.5	124	D	1.35
Sand	35	-	20	1.0	239	C	1.25
Gravel	44	-	21	1.0	401	B	1.25

In linear equivalent dynamic analyses, it is also necessary to introduce the variation of shear modulus G and damping ratio D with the shear strain level γ in the computational model. Therefore, the curves $G(\gamma)/G_0$ and $D(\gamma)$ for the three materials (Figure 2) have been assumed according to various literature indications:

- for clay, the curves suggested by Vucetic & Dobry (1991) for I_P=30% ;
- for sand, the well-known curves by Seed & Idriss (1970);
- for gravel, the relationships reported by Stokoe (2004) for D_{50} = 10mm.

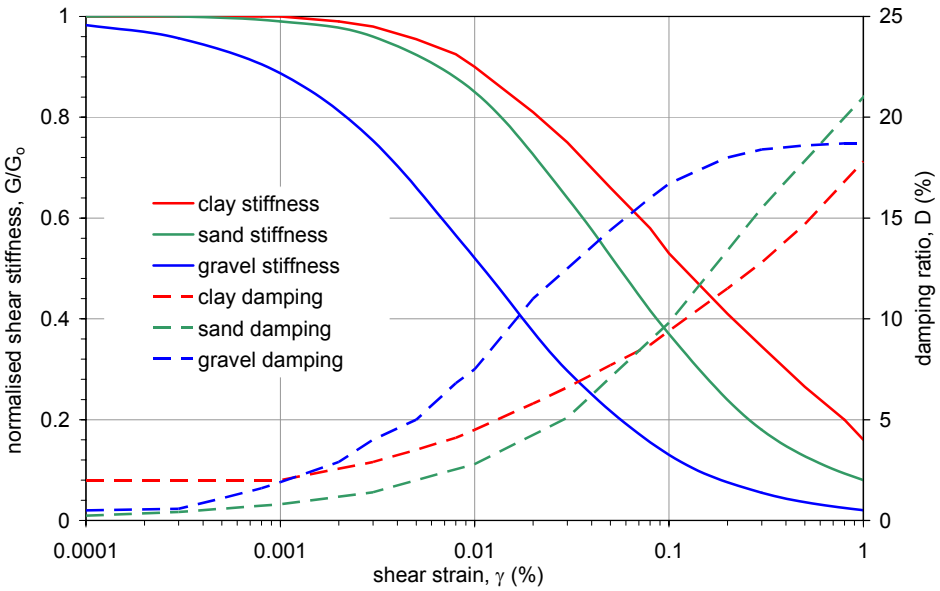

Figure 2. Variation of normalised stiffness and damping with shear strain level.

ANALYSIS OF THE TRANSVERSE SECTION

In a full dynamic analysis, the force increments in the lining due to an earthquake are directly obtained as an output of the numerical method adopted for the simulation of the shaking of the coupled ground-tunnel system. On the other hand, in simplified (pseudo-static or dynamic) methods the kinematic soil-structure interaction is neglected and the analysis is uncoupled: a displacement field is applied to the tunnel boundary, as obtained by means of a one-dimensional free-field site response analysis, i.e. by neglecting the effects of tunnel shape and stiffness on the seismic ground behaviour. Moreover, the effects of compression waves are also neglected, as only S waves are considered, which propagate in vertical planes inducing shear strain γ. Thereafter, deformations are used to calculate seismic force increments in the tunnel lining by means of closed-form elastic solutions, such as those by Penzien & Wu (1998).

Pseudo-static analysis

Four different methods have been developed, to evaluate the maximum shear stress, which can be calculated from the equilibrium of a deformable soil column between the surface and a given depth z. The maximum soil shear strain at a depth z is always calculated by dividing the maximum shear stress, $\tau_{max}(z)$, by the shear stiffness, G(z), at the same depth:

$$\gamma(z) = \frac{\tau_{max}(z)}{G(z)} \tag{3}$$

With each pseudo-static method, both linear and linear equivalent analyses have been carried out; in linear analyses the shear modulus G in Eq. (3) coincides with the small strain stiffness G_o, whereas in linear equivalent analyses it depends on the strain level as specified in Fig. 2. For a straightforward evaluation of the maximum shear strain in the soil, the Ramberg & Osgood (1943) model has been used, which expresses the shear strain as a function of the shear stress as follows:

$$\gamma_{max}(z) = \frac{\tau_{max}(z)}{G_0} + C\left[\frac{\tau_{max}(z)}{G_0}\right]^R \tag{4}$$

Method 1

It is assumed that the profile of peak acceleration with depth is harmonic, as the first modal shape of a homogeneous layer of soil on a rigid bedrock. The acceleration at the bottom of the layer ($a_{max,b}$) has been set at the value for outcropping rock, a_g, whereas the acceleration at surface ($a_{max,s}$) can be evaluated following the specifications of the Standards as:

$$a_{max,s} = Sa_g \tag{5}$$

where S is the site amplification factor (*cf* Tab. 1). Hence, the vertical profile of a_{max} is given by:

$$a_{max}(z) = a_g + \text{sen}\left[\frac{2\pi(H-z)}{4H}\right](a_{max,s} - a_g) \tag{6}$$

and the maximum shear stress is computed by integration as:

$$\tau_{max}(z) = \int_0^z \rho a_{max}(z)dz \tag{7}$$

Method 2
The second method assumes a different variation of a_{max} with depth: namely, the a(z) profile is assumed linear from surface (Sa_g) to bedrock (a_g). Such hypothesis corresponds to that of a layer of soil shaking in a range of frequencies much lower than the fundamental.

Method 3
The shear stress distribution with depth in Eq. (3) has been calculated according to the following equation of dynamic equilibrium of a soil column:

$$\tau_{max}(z) = r_d(z)\frac{a_{max,s}}{g}\sigma_v(z) \tag{8}$$

which is often used in the evaluation of liquefaction susceptibility. In Eq. (8), σ_v is the total vertical stress, and r_d is a reduction parameter which takes into account the soil column deformability. This latter can be calculated as a function of depth z, for instance through the relationships given by Iwasaki et al. (1978) and Liao & Whitman (1986), or eventually including the effects of magnitude, as suggested by Idriss & Boulanger (2004). Further values of $r_d(z)$ can be derived by the reduction factors of $a_{max,s}$ with depth given by Power et al. (1996). In this work the relationship by Iwasaki *et al.* (1978):

$$r_d = 1 - 0.015z \tag{9}$$

was considered as a first reference. In Eq. (9) the depth z is expressed in m.

Method 4
This method is similar to the previous, but the values of r_d have been calculated by using the equation:

$$r_d(z) = \frac{\tau_{max}(z)}{\sigma_v(z)a_{max,s}/g} \tag{10}$$

where τ_{max} was computed by the site seismic response (SSR) analyses described in the following sub-section. The value of $a_{max,s}$ was set again by using Eq. (5); this was necessary to provide results comparable with those obtained by the other methods.

In Fig. 4 the profiles of $r_d(z)$ according to Eq. (10), are compared with the profiles suggested by the above mentioned Authors. Computed profiles refer to design earthquakes with a_g increasing from 0.05g to 0.35g, corresponding to the four seismic categories as defined by the Italian code (OPCM 3274, 2003).

It is pointed out that the values r_d as derived by Eq. (10) are often higher than unity at the ground level, as ground accelerations computed in the analyses are usually higher than Sa_g. This agrees with recent works of Pitilakis et al. (2006) and Bouckovalas et al. (2006): in fact, by analysing several ground conditions, they obtained values of S higher than those suggested by OPCM 3274 and EC8.

The figure also shows that r_d increases as a_g decreases, thus indicating a noticeable effect of non-linearity. This effect is more evident close to the ground surface, where the shear stiffness undergoes more significant changes with depth. Despite the higher values predicted for surface motion, this method yields overall lower shear stresses at the tunnel depth with respect to the literature relationships, at least for the subsoil profiles considered.

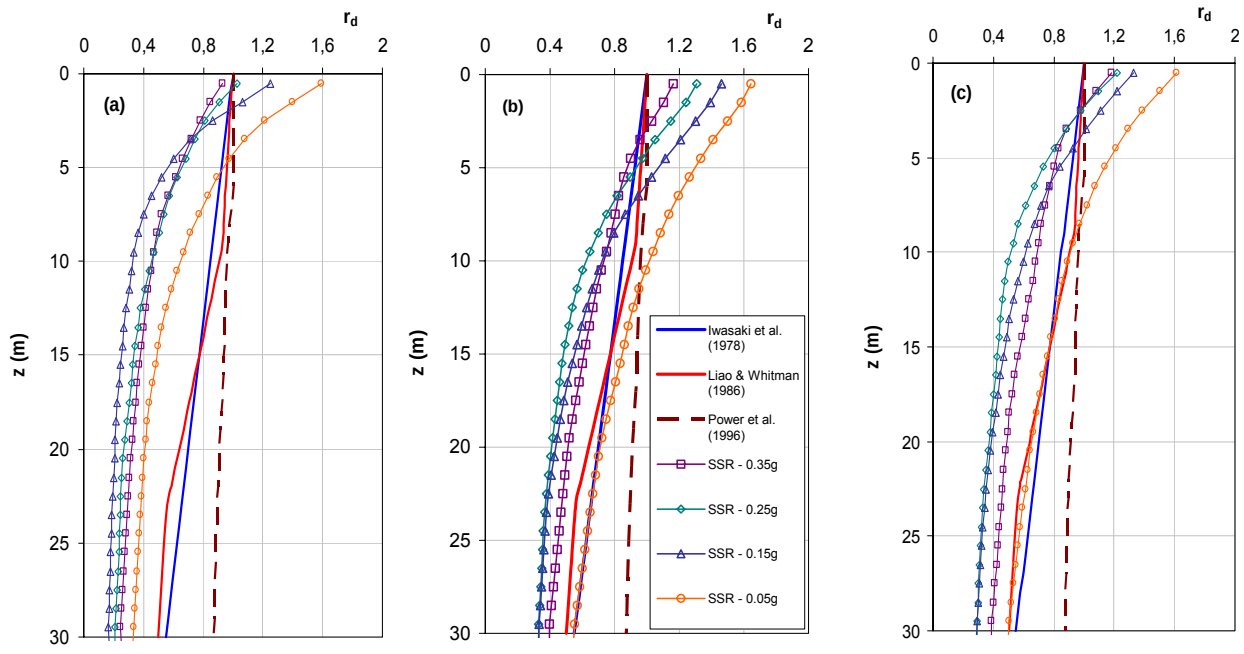

Figure 4. Profiles of $r_d(z)$ after literature and as computed with EERA for clay (a), sand (b) and gravel (c)

Simplified dynamic analysis

Acceleration, shear stress and strain induced by the seismic waves at the tunnel depth have been calculated through a free-field one-dimensional SSR analysis. In such a way, both the acceleration time history and the site characteristics are taken into account, whereas the kinematic soil-structure interaction is still neglected. Peak values of the average soil shear strain, γ_{ave}, in the range of depths between the tunnel crown and the invert have been computed. The SSR analyses have been performed by means of the code EERA (Bardet et al., 2000), which operates in the frequency domain. Ground conditions and soil behaviour have been modelled according to Figs. 1 and 2.

The input acceleration time histories have been selected from a database of records of Italian seismic events (Scasserra et al., 2006; Lanzo, 2006). The signals have been scaled to values of a_g equal to 0.05g, 01.5g, 0.25g and 0.35g (according to the seismic zonation specified by OPCM 3274, 2003), and have been applied to the base of the subsoil models.

Full dynamic analysis

The FE software Plaxis v8 (Brinkgreve, 2002) has been used to perform two-dimensional free-field and soil-structure interaction dynamic analyses. The code allows defining the damping tensor [C] through the Rayleigh formulation, i.e. as a linear combination of the mass tensor [M] and the stiffness tensor [K]:

$$[C] = \alpha[M] + \beta[K] \tag{11}$$

Coefficients α and β have been calculated according to the double frequency method, assuming that the damping ratio is constant between the first natural frequency of the deposit and a frequency n times larger; n is the first odd integer which approximates by excess the ratio between the fundamental frequency of the seismic signal and the first natural frequency of the deposit. This method avoids the overestimate of damping inside the considered frequency range (Lanzo et al., 2004). The bedrock has been assumed as a rigid boundary, whereas lateral mesh boundaries, about 10 D away from the tunnel side, are modelled as dampers according to the Lysmer & Kuhlmeyer (1969) formulation.

Results

An overview on the adopted methods is shown in Table 2, summarising the criteria used to evaluate the maximum acceleration at surface ($a_{max,s}$) and at the bedrock ($a_{max,b}$), the maximum shear stress τ_{max} and the corresponding strain amplitude γ_{max}.

Table 2: Overview on the methods of transverse section analysis.

Analysis	Method	$a_{max,b}$	$a_{max,s}$	τ_{max}	γ_{max}	
					Linear analysis	Linear equivalent analysis
Pseudo-static	method 1	a_g	S· a_g	Eq. (7)	τ_{max}/G_0	Eq. (4)
	method 2	a_g				
	method 3	(-)		Eq. (8), (9)		
	method 4	(-)		Eq. (8), (10)		
Simplified dynamic	EERA	a_g	free-field SSR analyses			
Full dynamic	Plaxis	a_g	soil structure interaction analyses			

Some representative results which have been obtained by applying the methods in Tab. 2 are shown in the following. A comparison between pseudo-static and simplified dynamic methods is shown in Figs. 5-6, in terms of vertical profiles of peak acceleration, shear stress and strain. These results refer to ground type C (sand), under a seismic event with a_{max}= 0.35g. The results of SSR analyses carried out with six different input signals have been plotted with depth (grey lines) and averaged (black lines).

It is worth noticing that, for linear soil behaviour (Fig. 5), the values assumed for a_{max} in the first two pseudo-static methods are lower than those calculated by SSR, at least from surface to the tunnel depth. Nevertheless, the values of τ_{max} result comparable, whereas the shear strain γ_{max} computed by methods 1 and 2 becomes even significantly higher. More evident differences are observed for linear equivalent analyses (Fig. 6), as all pseudo-static methods overestimate noticeably the values of γ_{max}.

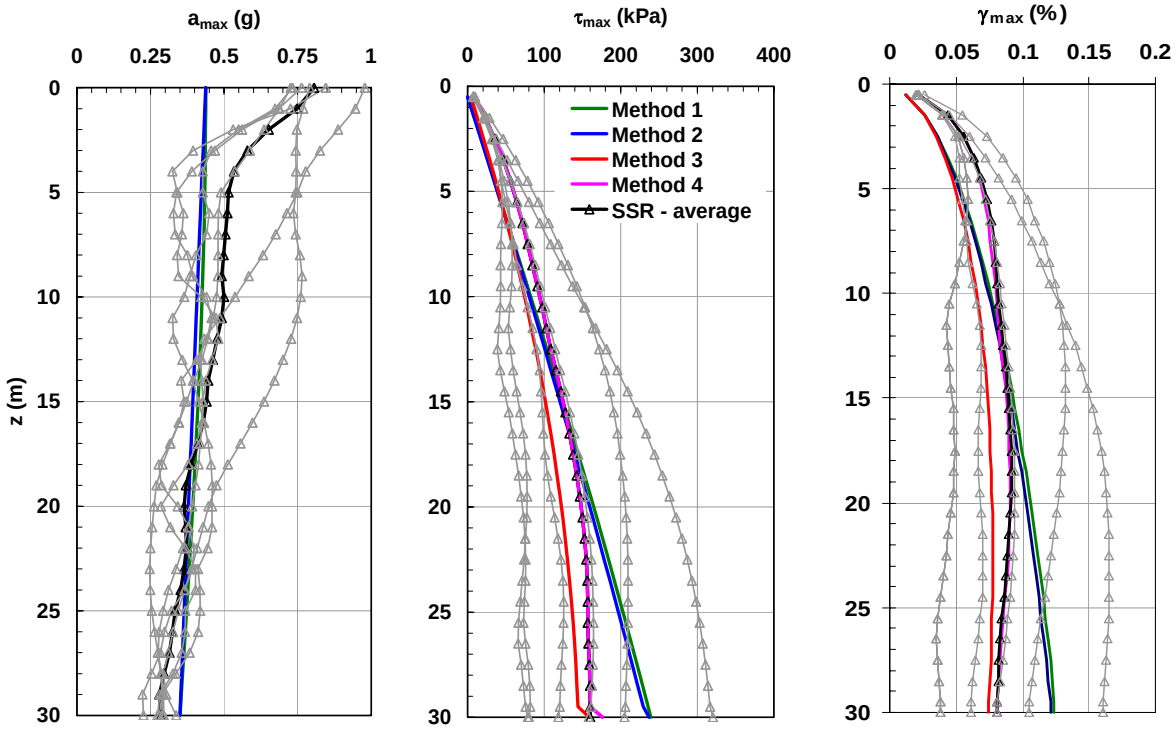

Figure 5. Profiles of $a_{max}(z)$, $\tau_{max}(z)$, $\gamma_{max}(z)$ for sand and a_g=0.35g: linear analyses.

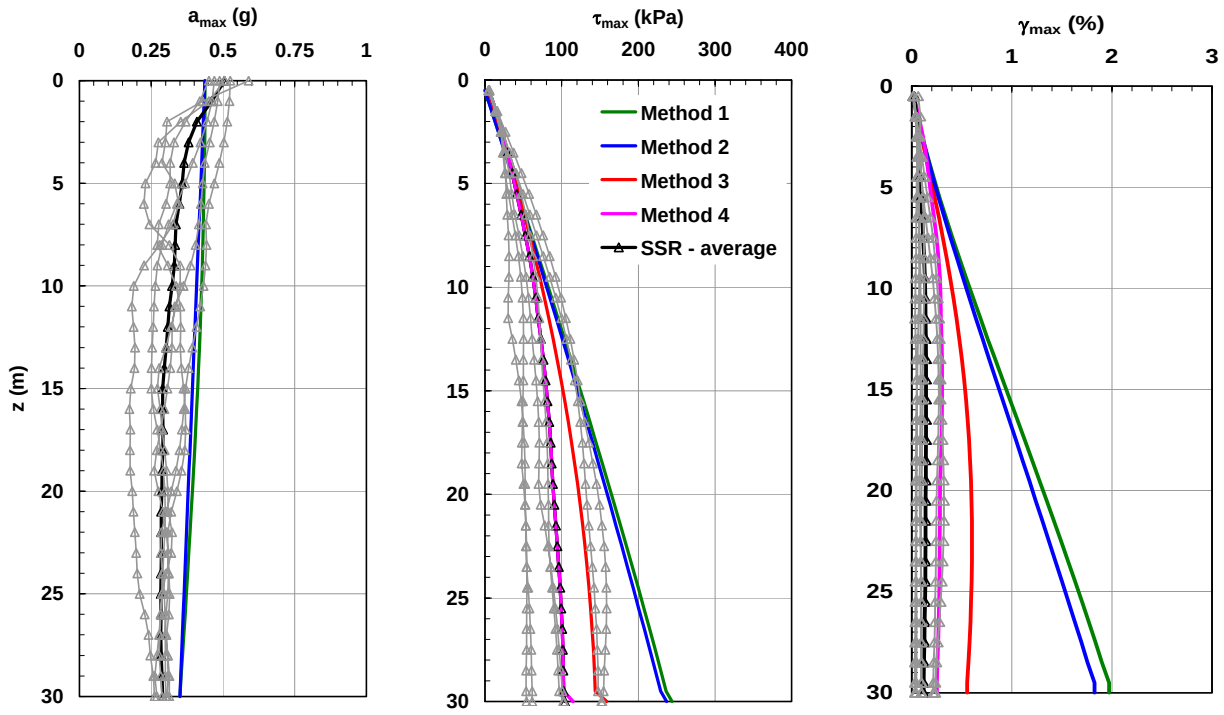

Figure 6. Profiles of $a_{max}(z)$, $\tau_{max}(z)$, $\gamma_{max}(z)$ for sand and a_g=0.35g: linear equivalent analyses.

In Figs. 7 a-b the ratio between the pseudo-static average strain, γ_{ps}, and the corresponding average value as computed by simplified dynamic SSR analyses, γ_{sd}, is plotted along the maximum reference acceleration a_g. The strain values considered are the average values between the depths corresponding to the crown and the invert of the tunnel.

The plots confirm that, in most cases, pseudo-static methods generally provide a higher average shear strain than simplified dynamic analysis, particularly for non-linear behaviour and for the case of the soft clay deposit. Nevertheless, some ratios for granular soil are lower than unity, thus indicating that pseudo-static analyses, in such cases, underestimate the shear strain and, therefore, forces in the lining. It can be summarised that pseudo-static analyses can result as more conservative in estimating the strain level, as the peak acceleration and the degree of soil non-linearity increase.

The comparison in Fig. 7 confirms that the methods 1 and 2 are in many cases too conservative, whereas the methods 3 and 4, and in particular the latter, yield predictions of the strain level closer to the simplified dynamic analysis.

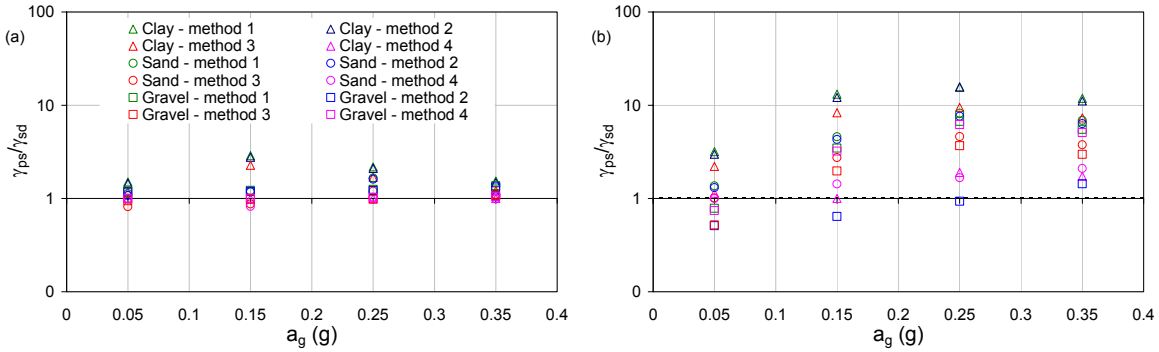

Figure 7. Ratios between shear strain calculated in the different pseudo-static methods and that in the simplified dynamic analysis: linear (a) and linear equivalent (b)

In Fig. 8 a comparison between free-field dynamic linear analyses in frequency (EERA) and in time domain (Plaxis) is shown, in terms of vertical profiles of peak variables for the sand subsoil (ground type C), subjected to three different acceleration time histories scaled to 0.35g. It can be noted that, on the average, the two dynamic analyses yield comparable results in terms of shear strain amplitudes at the tunnel depth.

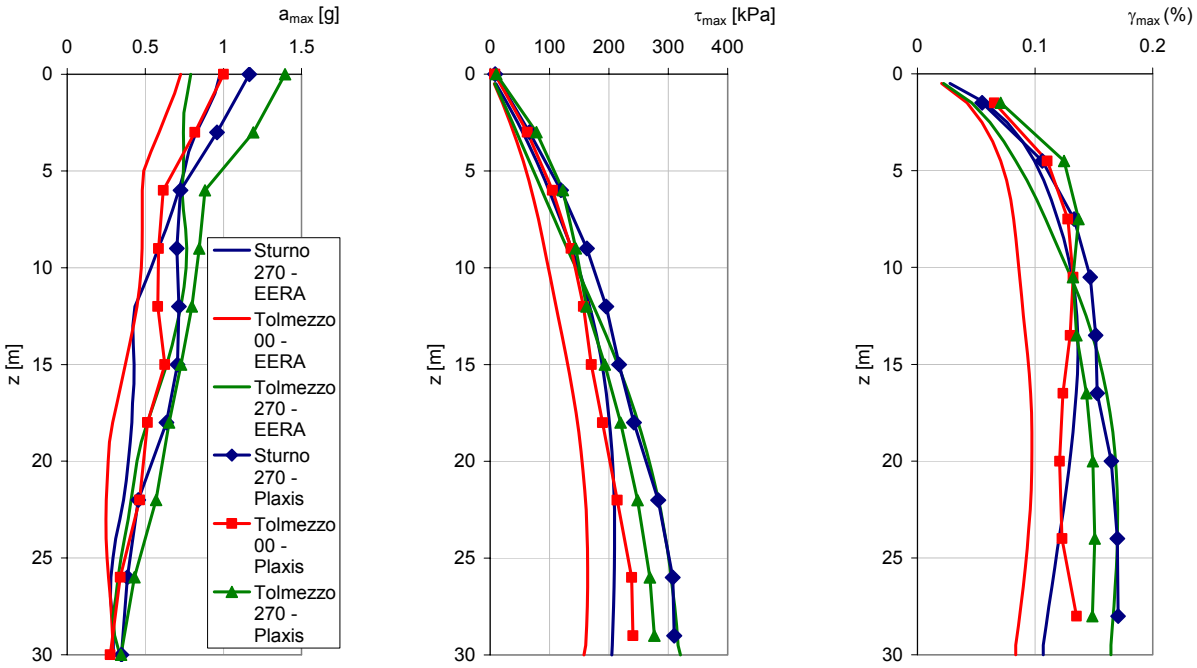

Figure 8. Profiles of $a_{max}(z)$, $\tau_{max}(z)$, $\gamma_{max}(z)$ for sand and a_g=0.35g: comparison between simplified dynamic analyses by EERA and Plaxis

For both pseudo-static and simplified dynamic analyses, it has been assumed that the internal forces in the lining can be calculated from the free-field average shear strain, i.e. neglecting the kinematic interaction between the lining and the ground. In this work, the analytical expressions by Penzien & Wu (1998) have been used, which refer to a tunnel with diameter D, and with a lining defined by a second moment of area I_t, and elastic parameters E_t and ν_t. The tunnel is surrounded by a homogeneous and isotropic half-space, with linear elastic parameters E and ν. Under the hypothesis of rough interface between the lining and the soil, the variation of thrust (N), shear force (T) and bending moment (M) with the angle θ is given by:

$$N(\theta)=\frac{24E_tI_t\Delta(\theta)}{D^3(1-\nu_t^2)} \qquad T(\theta)=\frac{24E_tI_t\Delta(\theta)}{D^3(1-\nu_t^2)}\tan 2\left(\theta+\frac{\pi}{4}\right) \qquad M(\theta)=\frac{6E_tI_t\Delta(\theta)}{D^2(1-\nu_t^2)} \tag{12}$$

where the distortion Δ is defined as follows:

$$\Delta(\theta)=\frac{2D\gamma_{ave}(1-\nu_t)}{1+\alpha_{st}}\cos 2\left(\theta+\frac{\pi}{4}\right) \qquad \alpha_{st}=\frac{48E_tI_t(1+\nu)(3-4\nu)}{D^3E(1-\nu_t)} \tag{13}$$

with γ_{ave} equal to either γ_{ps} or γ_{sd}. The plots of internal forces with the angle θ have been compared in Fig. 9 with the corresponding forces as computed by one of the full dynamic linear analyses (Sturno record), for the sand subsoil and a_g=0.35g. The comparison shows in this case the fair approximation achieved with the all the pseudo-static methods.. With respect to dynamic soil-structure interaction analyses, the simplified dynamic method provides fairly consistent values of shear force T and bending moment M, whereas it underestimates the thrust N. The latter result confirms the conclusions of a study by Hashash *et al.* (2005) about the use of Eq. (12) for predicting the thrust N.

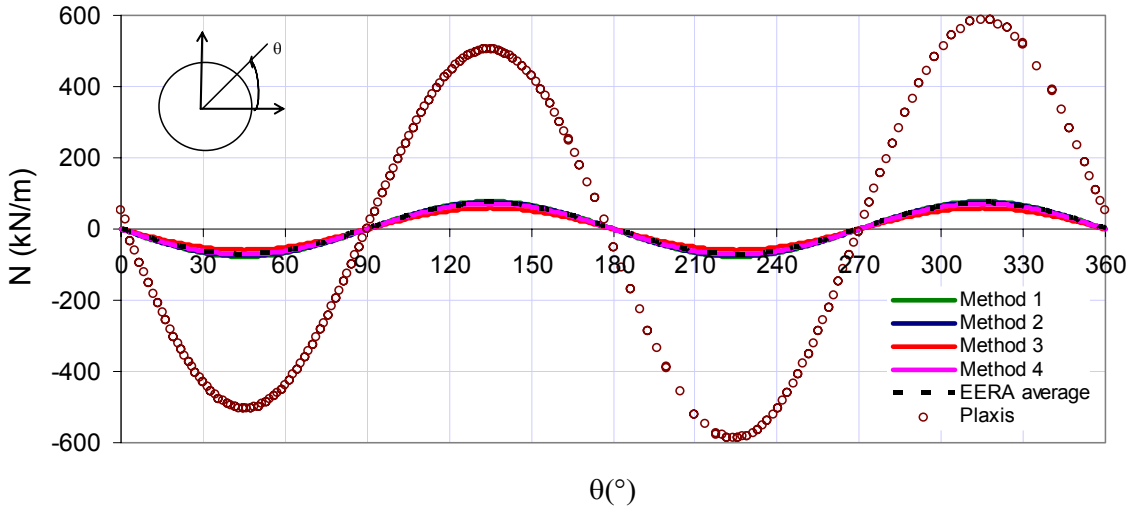

(a)

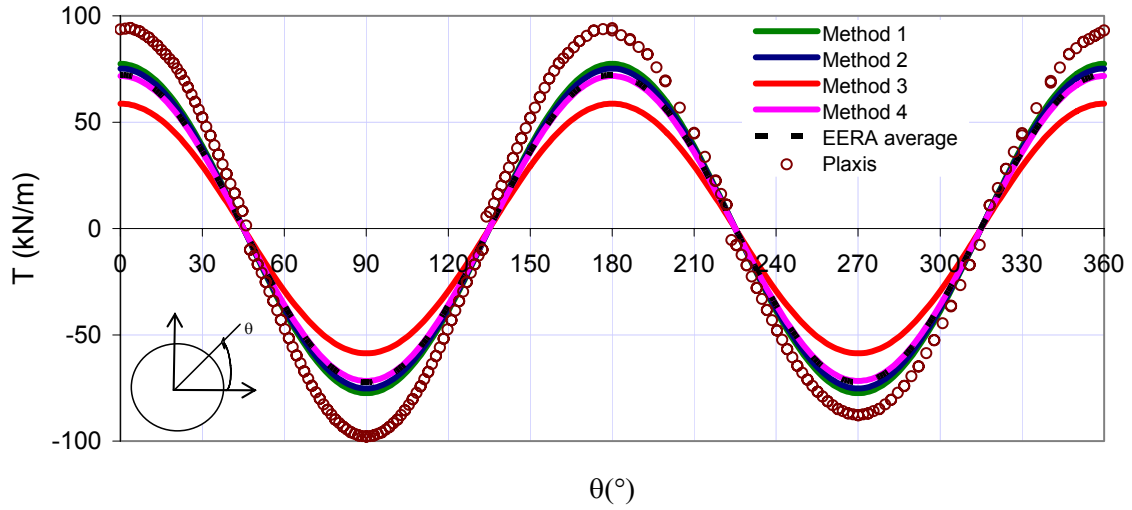

(b)

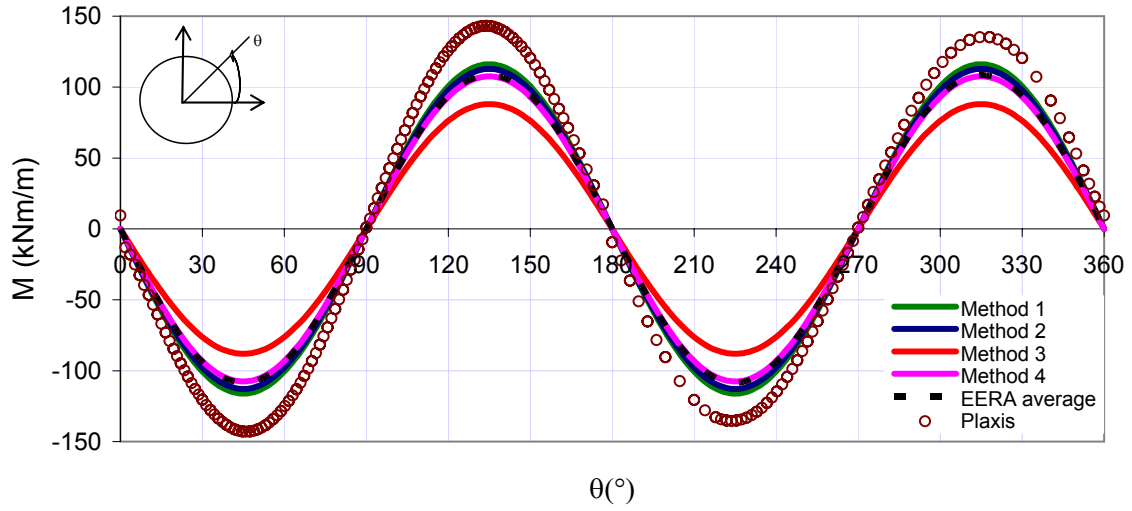

(c)

Figure 9. Forces in the lining: sand, a_g=0.35g, linear analysis

ANALYSIS ALONG TUNNEL AXIS

The seismic analysis of tunnel in longitudinal direction has been performed by two simplified methods which model the structure as a one-dimensional linear elastic beam:

1) finite difference solution of the dynamic equilibrium equation presented by Kawashima (2000)
2) approximate solution proposed by Fu et al. (2004)

Both methods require as an input the free-field ground displacement at the tunnel axis depth. To this purpose, the displacement profile associated with the first mode of linear elastic, homogeneous and isotropic layer of thickness H, overlying stiff bedrock, has been considered (Kawashima, 2000). Once that the maximum horizontal transverse displacement at the ground surface u_s is known, the horizontal transverse displacement at a given depth z, $u_g(z)$, can be therefore calculated as:

$$u_g(z) = \cos\left(\frac{\pi z}{2H}\right) u_s \tag{14}$$

The variation of the free-field displacement along the tunnel axis y, $u_{ff}(y,z)$, will be then given by:

$$u_{ff}(y,z) = u_g(z) \cdot \text{sen}\left(\frac{\pi}{2} + \frac{2\pi y}{\lambda_s}\cos\theta\right) \tag{15}$$

in which λ_s is the shear wavelength and θ the angle defining the direction of propagation of the incident waves with respect to the axis y. It is worth noticing that Eq. (15) takes into account, in a simplified way, both the obliquity of seismic waves and the non-synchronism of the motion along the longitudinal axis. The following expression can be used to evaluate λ_s:

$$\lambda_s = \frac{2 L_1 L_2}{L_1 + L_2} \tag{16}$$

where the two wavelengths L_1 and L_2 are given by:

$$L_1 = T_s \bar{V}_s \quad L_2 = T_s V_r \tag{17}$$

being the period T_s expressed as follows:

$$T_s = 1.25 \sum_{i=1,n} \frac{4 h_i}{V_{si}} \tag{18}$$

In Eqs. (17)-(18), $\bar{V}_s$ is the average value of the shear wave velocity in the soil, V_r is the shear wave velocity in the bedrock, n is the number of sub-layers in which the deposit has been subdivided, h_i and V_{si} are the thickness and the shear wave velocity of the i-th sub-layer, respectively.

Evaluation of displacements

In this work, the surface displacement u_s in Eq. (14) has been calculated using three different pseudo-static procedures (PS) and one simplified dynamic method (SD).

Method PS 1

The peak surface horizontal displacement is calculated from the spectral velocity S_v at bedrock and the fundamental period of the deposit T_s, through the expression suggested by Kawashima (2000):

$$u_s = \frac{2T_s}{\pi^2} S_v(T_s) \tag{19}$$

where T_s is provided by Eq. (18), and S_v has been evaluated from the design acceleration spectrum S_a as defined by OPCM 3274 (2003), by setting S=1.

Method PS 2
The second method is based on Eq. (19), but $S_v(T_s)$ has been evaluated as the average spectrum deduced from the selected acceleration time histories.

Method PS 3
In this method the maximum displacement at surface (in cm) is given by the equation:

$$u_s = 2.5 \cdot S \cdot T_C \cdot T_D \cdot a_g \tag{20}$$

where T_C and T_D are the values of the period defining the design spectrum of OPCM 3274 (2003).

Method SD
This method is based on a simplified dynamic analysis for the free-field site seismic response, aimed to calculate the earthquake-induced maximum displacements of the soil in the range of depths corresponding to the tunnel section. Therefore, in this case the values of $u_g(z)$ could be obtained easily from the same free-field SSR analyses adopted for the study of the transverse section.

Figure 10 shows a comparison of the four methods, in terms of the horizontal displacement obtained with Eq. (14) for each of the aforementioned pseudo-static methods, $u_{g,PS}$, divided by the corresponding displacement, $u_{g,SD}$, calculated by averaging the results of the linear dynamic analyses. Again, it can be noted that the pseudo-static methods always predict higher displacements with respect to the SSR; more in detail, method PS3 appears too much conservative, while method PS2 gives the closest approximation to the dynamic simplified analysis.

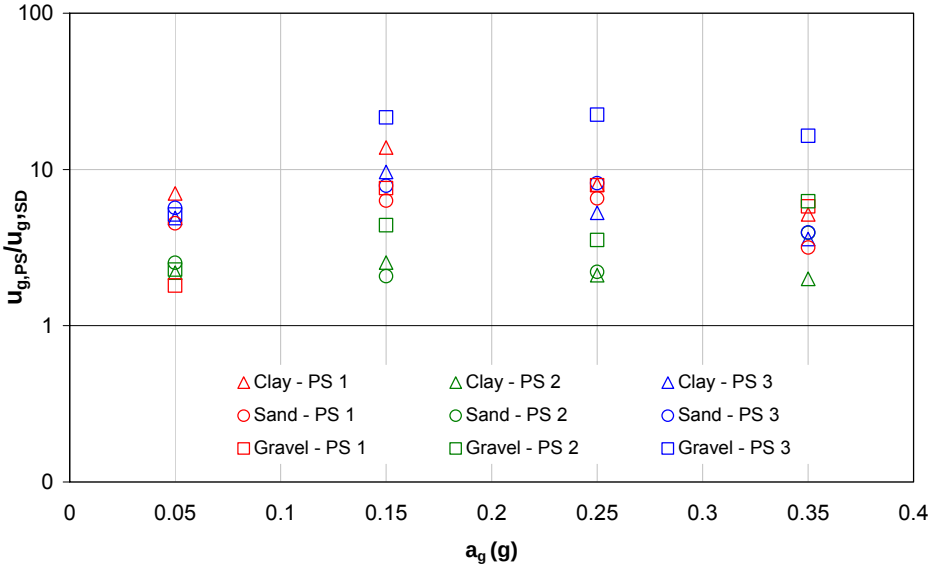

Figure 10. Comparison between pseudo-static and simplified dynamic prediction of u_g

Finite difference solution

Forces in the tunnel lining have been calculated by modelling the tunnel as an elastic beam on Winkler's springs. By neglecting the inertial effects (Okamoto et al., 1973), the differential equation governing the pseudo-static flexural response of the beam is (Kawashima, 2000):

$$EI\frac{\partial^4 u(y)}{\partial y^4} = K_t\left[u_{ff}(y) - u(y)\right] \tag{21}$$

Eq. (21) has to be solved together with the boundary conditions, expressed in terms of displacement and its derivatives, which correspond to setting zero values of shear force, T, and bending moment, M, at the beam ends. In Eq. (21), u(y) is the structure displacement, $u_{ff}(y)$ is the free-field soil displacement as calculated by Eq. (15), EI is the flexural stiffness of the beam, and K_t is the soil-equivalent spring stiffness. This latter may be evaluated by the expression (St.John & Zahrah, 1987):

$$K_t = \frac{16\pi G_{ave}(1-\nu_s)}{(3-4\nu_s)}\left(\frac{D}{\lambda_s}\right) \tag{22}$$

where G_{ave} is a mean value of the soil shear modulus at small strains, ν_s is the soil Poisson's ratio. The solution to Eq. (21) has been achieved numerically using a finite difference method (Valentino, 2006), which allows the eventual variability of K_t along the tunnel axis to be readily accounted for.

Approximate solution

The procedure proposed by Fu et al. (2004) allows determining the tunnel deformation without solving Eq. (21). In fact, the tunnel deformation u(y) is calculated by multiplying the free-field displacement at the tunnel axis depth, $u_{ff}(y)$, by a reducing factor R defined as:

$$R = \frac{u(y)}{u_{ff}(y)} = \frac{1}{1+\frac{EI_{eq}}{K_t}\left(\frac{2\pi}{\lambda_s}\right)^4} \tag{23}$$

where λ_s and K_t are given by Eq. (15) and (22) respectively, and EI_{eq} is the flexural stiffness of a beam with a rectangular section equivalent to the real transverse tunnel section. The values of R for the cases under consideration are shown in Table 3, together with other calculation parameters. It is worth noticing that for all subsoil models, notwithstanding the wide variability of λ_s and K_t, the computed values of R are very close to unity. This means that the tunnel is very flexible compared to the soil, therefore the kinematic interaction effects result negligible.

Table 3: Values of factor R and other model parameters

ground	ν_s	G_{ave} (MPa)	λ_s (m)	K_t (MN/m)	R
clay	0.50	28.2	260	11.9	0.977
sand	0.30	115.5	231	54.8	0.992
gravel	0.23	344.2	200	188.9	0.997

Results

An example of comparison in terms of shear force and bending moment as obtained by the two procedures is shown in Fig. 11a-b. The results refer to the sand deposit excited by a seismic input with peak acceleration of 0.35g; the displacement $u_g(z)$ has been evaluated by SSR (method SD).

It can be observed that the calculated forces differ only nearby the ends of the tunnel. It should be noted that the solution proposed by Fu et al. (2004) does not account for the boundary conditions,

which on the contrary are included in the finite difference solution. Along the tunnel body, the two methods provide essentially the same results.

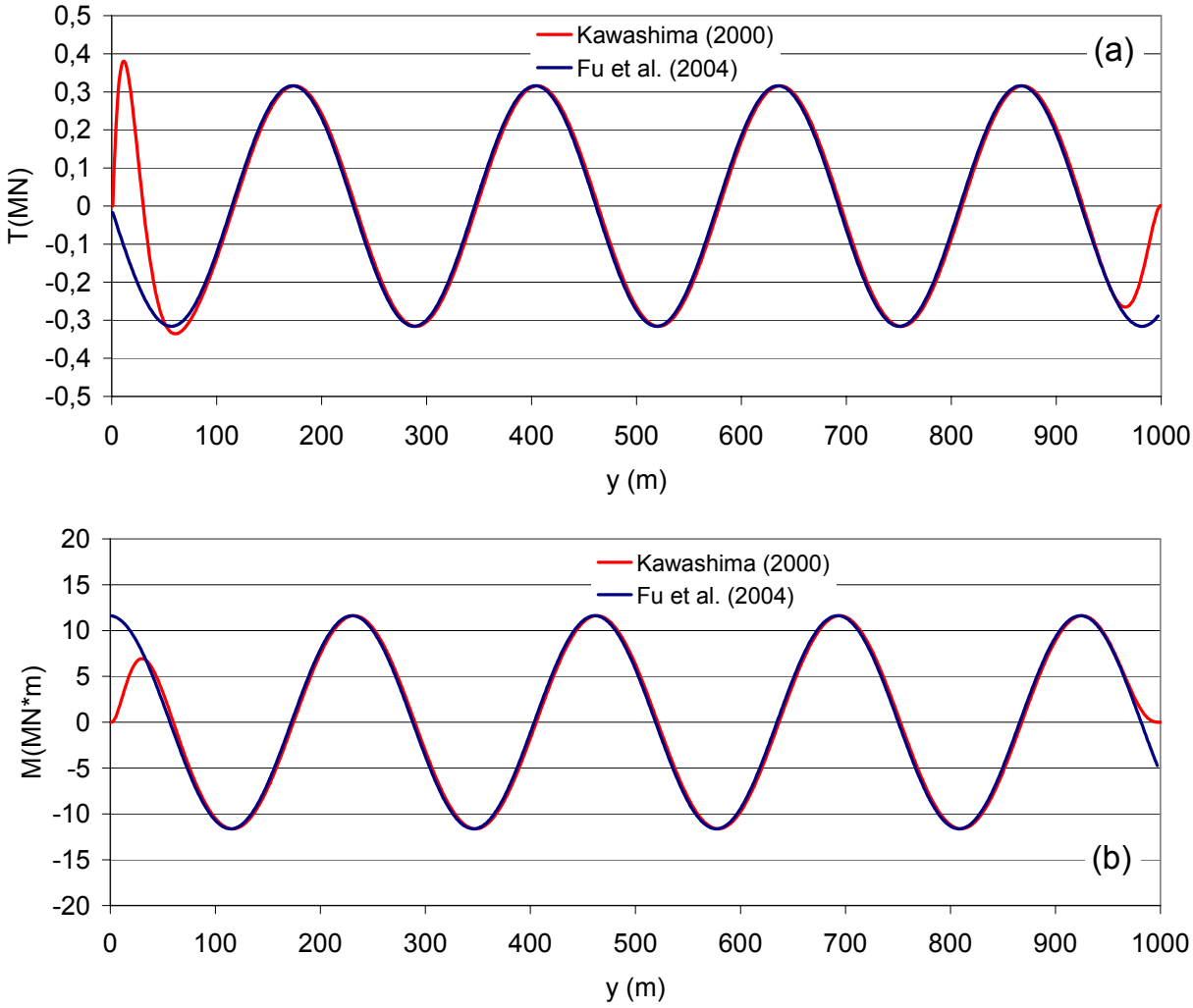

Figure 11. Shear forces (a) and bending moments (b) calculated using the procedures by Kawashima (2000) and Fu et al. (2004).

CONCLUDING REMARKS

Engineering predictions of the load increments induced by an earthquake in a tunnel lining can be accomplished following three different design approaches, corresponding to increasing levels of complexity in analytical models, soil characterisation and description of seismic input:

- Pseudo-static analysis, where the seismic input is reduced to equivalent inertia force or peak strain amplitude, computed through a free-field ground pseudo-static analysis, and then considered acting on the tunnel lining in static conditions as well.
- Simplified dynamic analysis, where the soil straining is computed through a dynamic free-field seismic response analysis, and then applied to the tunnel section or axis, again in pseudo-static conditions, eventually accounting for the kinematic tunnel-soil interaction in a simplified way.
- Full dynamic analysis, where the soil and tunnel responses are mechanically coupled and analysed via numerical modelling, such as dynamic finite element or finite difference methods.

In this paper, the different levels of analysis have been developed on idealised geometry and soil conditions, considered representative of soil classes specified by the new Italian seismic code. Linear and non-linear analyses along the transversal and longitudinal directions were carried out with different methods, and the results have been described and compared.

The force increments as calculated with the different procedures in the transverse section have been compared, showing a fair approximation to the full dynamic analysis achieved with the simplified uncoupled approach, as far as the tunnel lining is reasonably flexible. In the future, the reliability of pseudo-static analysis may be improved with more specific simplified functions expressing the soil deformation as a function of depth.

In the longitudinal direction, two procedures have been used, which can take into account, in a simplified way, both the angle of incidence of seismic waves and the non-synchronism of the motion. A comparison in terms of computed shear force and bending moment gave indication that in the examined case, where the tunnel stretch is relatively flexible compared to the soil, the two approaches yield essentially the same results at distance from the tunnel ends. However, both approaches need to be further tested with stiffer tunnel structures and against full dynamic interaction analyses.

ACKNOWLEDGEMENTS

This work is a part of a Research Project funded by ReLUIS (University Network of Seismic Engineering Laboratories) Consortium. The Authors wish to thank the coordinator, prof. Stefano Aversa, for his continuous support and the fruitful discussions. The strong motion database utilized in this study was developed as part of an ongoing joint project involving researchers from the University of Rome La Sapienza and the University of California, Los Angeles, with support from the Pacific Earthquake Engineering Research Center. Preliminary results from this group were reported by Scasserra et al. (2006), but the data utilized here have not been published.

REFERENCES

Bardet J. P., Ichii K., and Lin C. H., “EERA a Computer Program for Equivalent-linear Earthquake site Response Analyses of Layered Soil Deposits”, Univ. of Southern California, Dep. of Civil Eng., 2000

Bilotta E., Aiello V., Conte E., Lanzano G., Russo G., Santucci de Magistris F., and Silvestri F., “Sollecitazioni indotte da sisma in gallerie circolari interrate”, Proc. of V IARG, Pisa, 2006 (in Italian)

Bouckovalas G.D., Papadimitriou A.G., and Karamitros D., “Compatibility of EC-8 ground types and site effects with 1-D wave propagation theory”, Proceedings ETC-12 Workshop, NTUA Athens, 2006

Brinkgreve R.B.J., Plaxis 2D version8. A.A. Balkema Publisher, Lisse, 2002

d’Onofrio A., and Silvestri F., “Influence of micro-structure on small-strain stiffness and damping of fine grained soils and effects on local site response”, Proc. IV Int. Conf. on ’Recent Advances in Geothecnical Earthquake Engineering and Soil Dynamics’. San Diego, Paper 1.19, 2001

EN 1998-1, Eurocode 8: Design of structure for earthquake resistance,. Part 1: General rules, seismic actions and rules for buildings. CEN European Committee for Standardisation, Bruxelles, Belgium, 2003

Fu P.C., Wang G., and Zhang J.M., “Analytical approaches for underground structures subjected to longitudinally propagating shear waves”, Proc. V ICSDEE & III ICEGE, Berkeley, USA, 2004

Hashash, Y.M.A., Hook, J.J., Schmidt, B., and Yao, J.I-C., “Seismic design and analysis of underground structures”, Tunnelling and Underground Space Technology, 16, 247-293, 2001

Hashash, Y.M.A., Park D., and Yao J.I-C., “Ovaling deformations of circular tunnels under seismic loading, an update on seismic design and analysis of underground structures”, Tunnelling and Underground Space Technology, 20, 435-441, 2005

Idriss I.M., and Boulanger R., "Semi-empirical procedures for evaluating liquefaction potential during earthquakes", Proc. V ICSDEE & III ICEGE, Berkeley, USA (1) 32 -56, 2004

Iwasaki T., Tatsuoka F., Tokida K., and Yasuda S. "A practical method for assessing soil liquefaction potential based on case studies at various sites in Japan", Proc. II Int. Conf. on Microzonation, San Francisco, 1978

Kawashima K., "Seismic design of underground structures in soft ground: a review", Geotechnical Aspects of Underground Construction in Soft Ground, Kusakabe, Fujita & Miyazaki (eds). Balkema, Rotterdam, 2000

Lanzo G., "Database di accelerogrammi naturali italiani", Report of Task 6.3 'Slope stability', ReLUIS Consortium, 2006 (in italian).

Lanzo G., Pagliaroli A., D'Elia B., "Influenza della modellazione di Rayleigh dello smorzamento viscoso nelle analisi di risposta sismica locale", Proc. XI Italian National Conference on "L'ingegneria Sismica in Italia", 2004 (in Italian)

Liao S.S.C., and Whitman R.V., "Overburden correction factors for SPT in sand", Journal of Geotechnical Engineering, ASCE, 112(3):373-377, 1986

Lysmer J. and Kuhlmeyer R.L, "Finite dynamic model for infinite media", J. of Eng. Mech. Div., ASCE: 859-877, 1969

Okamoto S., Tamura C., Kato K., and Hamada M., "Behaviour of submerged tunnels during earthquakes", Proc. V World Conference on Earthquake Engineering, Rome, 1:544-553, 1973

OPCM 3274, "Primi elementi in materia di criteri generali per la classificazione sismica del territorio nazionale e di normative tecniche per le costruzioni in zona sismica", Gazzetta Ufficiale della Repubblica Italiana, n. 105-8/5/03, 2003

Owen G.N., and Scholl R.E., "Earthquake engineering of large underground structures", Report no. FHWA/RD-80/195. Federal Highway Administration and National Science Foundation, 1981

Pakbaz M., and Yareevand A., "2-D analysis of circular tunnel against earthquake loading", Tunnelling and Underground Space Technology, 20, 411-417, 2005

Penzien J., and Wu C.L., "Stresses in linings of bored tunnels", Earthquake engineering and structural dynamics, 27:283-300, 1998

Pitilakis K., Gazepis Ch, and Anastasiadis A., "Design response spectra and soil classification for seismic code provisions", Proceedings ETC-12 Workshop, NTUA Athens, 2006

Power M.S., Rosidi D., and Kaneshiro J., Vol.III "Strawman: screening, evaluation and retrofit design of tunnels", Report Draft, National Center for Earthquake Engineering Research, Buffalo, New York. 1996

Ramberg W., and Osgood W.R., "Description of stress-strain curves by three parameters", Technical Note 902, National Advisory Committee for Aeronautics, Washington, D.C. 1943

Rampello S., "Costruzioni in sotterraneo e scavi a cielo aperto", Chap. 15 in 'Aspetti geotecnici della progettazione in zona sismica - Linee Guida AGI', Associazione Geotecnica Italiana, Patron, Bologna, 2005 (in Italian)

Santucci de Magistris F., "Fattori di influenza sul comportamento meccanico dei terreni", App. B in 'Aspetti geotecnici della progettazione in zona sismica - Linee Guida AGI', Associazione Geotecnica Italiana, Patron, Bologna, 2005 (in Italian)

Scasserra G., Lanzo G., Mollaioli F., Stewart J.P., Bazzurro P., and Decanini L.D., "Preliminary comparison of ground motions from earthquakes in Italy with ground motion prediction equations for active tectonic regions", Proc. of the 8th U.S. National Conference on Earthquake Engineering, San Francisco, 2006

Seed H.B., and Idriss I.M., "Soil moduli and damping factors for dynamic response analysis", Report No. EERC70-10, Earthquake Engineering Research Center, Univ. of California, Berkeley, (California), 1970

St. John C.M., and Zahrah T.F., "Aseismic design of underground structures", Tunneling and Underground Space Technology, 2 (2), 165-197, 1987

Stokoe K.H., "Comparison of Linear and Nonlinear Dynamic Properties of Gravel, Sand, Silts and Clays", Proc. V ICSDEE & III ICEGE, Berkeley, USA, 2004

Valentino M., "Metodi dinamici e pseudostatici per l'analisi sismica di infrastrutture interrate", M.Sc. Thesis, University of Calabria, 2006 (in Italian)

Vanzi I., “Elastic and inelastic response of tunnels under longitudinal earthquake excitation”, Journal of Earthquake Engineering, Imperial College Press, United Kingdom, vol.4(2), 2000

Vucetic M., and Dobry R., “Effects of the soil plasticity on cyclic response”, Journal of Geotechnical Engineering, ASCE, 117(1):89-107, 1991

Wang J., “Seismic Design of Tunnels: A Simple State-of-the-art Design Approach”, Monograph 7, Parsons, Brinckerhoff, Quade and Douglas Inc, New York, 1993